Publishing House
AKAPIT

COMPUTER METHODS IN MATERIALS SCIENCE

Informatyka w Technologii Materiałów

Vol. 10, 2010, No. 3

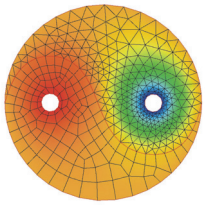

SELECTION OF THE THERMOMECHANICAL PROCESSING PARAMETERS OF CuCr FORGINGS

ROMAN KUZIAK[1], VALERIY PIDVYSOTS'KYY[1], MACIEJ PIETRZYK[2]*

[1] *Instytut Metalurgii Żelaza, ul. K. Miarki 12, 44-100 Gliwice, Poland*
[2] *Akademia Górniczo-Hutnicza, al. Mickiewicza 30, 30-059 Kraków, Poland*
**Corresponding Author: Maciej.Pietrzyk@agh.edu.pl*

Abstract

Accounting for the microstructure evolution in the design of technology for manufacturing of parts made of Cu based alloys is the objective of the paper. The particular emphasis is put on the CuCr alloys. The general information regarding properties of these alloys are given. Thermal, electrical and mechanical properties are presented and compared with those of pure copper and steel. Investigation of the role of aging and precipitation in hardening of the CuCr alloys is a particular objective of this work. Plastometric tests and stress relaxation tests were performed at various temperatures and various strain rates with different preheating schedules. The latter allows investigation of the effect of the initial microstructure on the flow stress. Rheological model and the model of microstructure evolution and precipitation kinetics are described and validated in the paper. The models are implemented into the finite element (FE) code and the microstructure, as well as mechanical properties of final products, are predicted. The combined FE-microstructure evolution model allows analysis of various variants of the manufacturing cycles composed of different preheating schedules, hot forging, cold forging and aging.

Key words: Copper-chromium alloys, microstructure evolution, precipitation, modelling

1. INTRODUCTION

Tendency to increase strength-to-density ratio will be for many years probably the main objective of research on materials processing. This objective is usually reached in two ways, either by design of new materials (chemical composition), or by control of microstructure through thermo-mechanical treatment during plastic deformation and heat treatment after de-formation. Due to its high density and low strength, copper is not competitive in this area comparing to other materials. On the other hand, there are several applications of materials, in which other beyond strength properties are important, such as electrical or thermal or corrosion resistance. Elements of electric circuits or heat exchangers are examples of applications, in which copper is an excellent material.

There are, however, several examples of thermal or electrical applications, which require certain reasonably high level of strength, not reachable by pure copper. This is the reason that some small quantities of other elements are added to copper to increase the strength, while high thermal and electrical properties are maintained. Copper-1% chromium, which is investigated in the present work, is an example of such material. Application of modelling to design the best manufacturing technology for this alloy is presented by Pietrzyk et al. (2010a; 2010b). Several variants of manufacturing chains are considered in Pietrzyk et al.'s paper (2010b) and such parameters as hardness of product, tool wear and costs of production are used as criteria for the selection of the

ISSN 1641-8581

best variant. Propsition of such a variant is given in Pietrzyk et al.'s work (2010b). The objective of the present work is investigation of the microstructure evolution during this selected manufacturing process and enabling to include the product microstructure to the optimization criterion.

2. CuCr ALLOYS

2.1. Properties and applications

Majority of typical applications of the CuCr alloys is connected with its high thermal and electrical properties, as well as with corrosion resistance (Report, 1998). Such applications as electrodes for resistance welding (Kumar & Singh, 2007), heat exchangers, tools for pressure casting, sparkless tools working in fire dangerous environments, electric contacts working under mechanical loads etc. should be mentioned. All these applications require certain level of strength and/or wear resistance, which exclude pure copper. Comparison of the basic properties of steel, pure copper and CuCr alloys in various working conditions is given in table 1. Chemical composition of the alloy investigated in the present work is given in table 2. It is seen in table 1 that small amount of chromium improves noticeably mechanical properties of the alloy while thermal and electrical properties are only slightly lower than those for pure copper. Beyond this, properties of the CuCr alloy depend strongly on the preceding heat treatment and mechanical treatment.

Table 1. *Selected properties of steel, pure copper and CuCr alloy. Notation: Re – yield stress, Rm – tensile strength, A_5 – elongation in the tensile test, HV – hardness, k – heat conduction, γ – electrical conductivity, SupSat - supersaturation.*

Material – state		*Re* MPa	*Rm* MPa	A_5	*HV* Kg/mm^2	*k* W/mK	γ MS/m
C-Mn steel	Annealed	120-220	260-350	30-40	60-98	49-55	6-8
Cu	Annealed	25-40	210-240	40-60	≈ 40	391	59.6
CuCr	Cast	65-85	200-230	34-48	≈ 60	65-85	171-324
	Hot forged	130-150	260-270	39-43	63-73	130-150	
	After SupSat	65-100	200-250	37-48	57-76	65-100	
	After aging	290-340	400-450	24-26	140-160	290-340	

Tablica 2. *Chemical composition (wght pct) of the investigated Cu-Cr alloy.*

As	Bi	Cr	Fe	Ni	Cu
< 0.001	< 5 ppm	0.81	0.026	< 0.001	balance

2.2. Rheological model

Plastometric tests were performed for the CuCr alloy with the chemical composition in table 2. The material was cast (ϕ 200 mm) and hot extruded to the diameters of 60-90 mm and then cooled in air. The average grain size after cooling was 15.6 μm. All the tests were performed on the Gleeble 3800 simulator at the Instytut Metalurgii Żelaza in Gliwice. The axisymmetrical samples measuring ϕ10×12 mm were compressed at temperatures 700-1000°C and strain rates 0.1-50 s^{-1} with the total strain of 1. Full set of the results of the tests is given in by Pietrzyk and Kuziak (2009).

Different preheating schedules before the tests were applied. It allowed investigation of the effect of the initial microstructure on the flow stress. After analysis in Pietrzyk et al.'s work (2010b) the following schedule was selected for the further analysis: heating to 950°C with the rate of 3°C/s, maintaining at 950°C for 300 s, cooling to the test temperature with the rate of -5°C/s, maintaining at the test temperature for 60 s and deformation. Inverse analysis (Szeliga et al., 2006) of the tests results yielded the flow stress vs. strain relation independent of the inhomogeneities of strains and temperatures in the tests. The flow stress equation proposed by Gavrus et al. (1996) was applied:

$$\sigma_p = \sqrt{3}\left[kq\, R\varepsilon^n + (1-R)k_{sat}q_{sat}\right]\left(\sqrt{3}\dot{\varepsilon}\right)^m \quad (1)$$

where:

$$R = \exp(-w\varepsilon) \qquad q = \exp\left(\frac{Q}{RT}\right)$$

$$q_{sat} = \exp\left(\frac{Q_{sat}}{RT}\right)$$

and k, k_{sat}, Q, q_{sat}, m, n, w – coefficients.

Due to problems with evaluation of the constant strain rate sensitivity m for the whole range of temperatures, linear relation of this coefficient on temperature is introduced:

$$m = a + b\left[0.002(T-273)-1\right] \quad (2)$$

where: T – temperature in K, R – universal gas constant, a, b – coefficients.

Coefficients in the flow stress model obtained from the inverse analysis are given in table 3.

Table 3. *Coefficients in equations (1) and (2) obtained from the inverse analysis.*

k	n	Q	k_{sat}	Q_{sat}	w	A	b
20.76	0.356	12030	0.889	29950	2.49	0.256	0.077

2.3. Microstructure evolution

Microstructure after the plastometric tests was analyzed. All samples were quenched after the deformation and the micrographs were taken. Selected microstructures are shown in figure 1. More results of the microstructure analysis are given in Pietrzyk et al.'s work (2010b). The main conclusions from this analysis are given below. In the deformation temperature range 800-900^{o}C, the microstructure of the samples is partly recrystallized. If recrystallized grains only are considered in the quantitative analysis, the recrystallized volume fraction increases with increasing temperature at which deformation is conducted (figure 2).

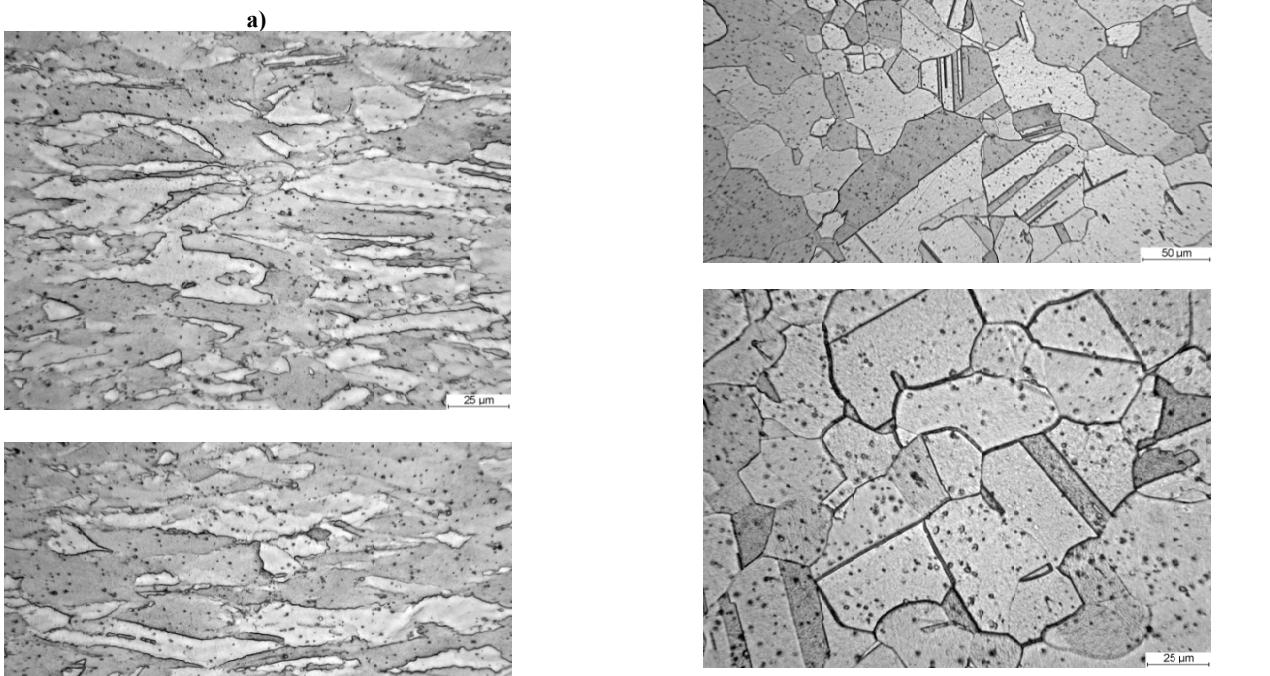

Fig. 1. *Micrographs of the CuCr samples deformed at 800^{o}C (a), 900^{o}C (b), 1000^{o}C (c) followed by water cooling; strain rate 1 s^{-1} (left) and 50 s^{-1} (right).*

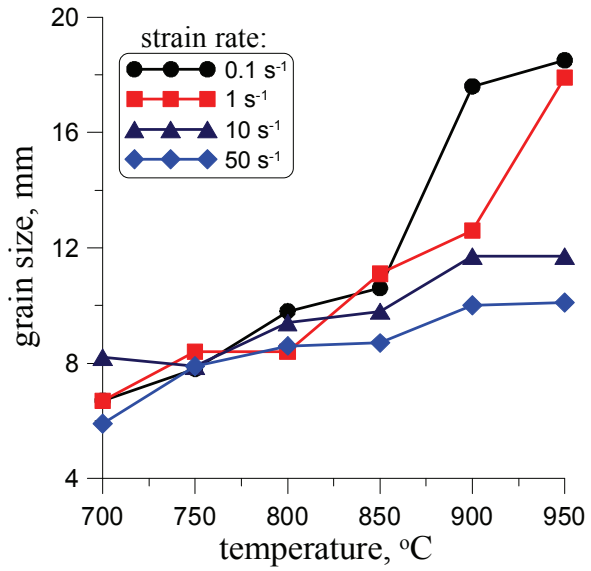

Fig. 2. *Grain size after plastometric tests as function of temperature and strain rate.*

For constant temperature, the grain size decreases slightly with increasing strain rate, what is a characteristic feature for dynamically recrystallized microstructures. However, this relation is not so clear and some deviations from this tendency are observed in figure 2, which may be due to experimental error. Influence of temperature and strain rate is small for lower temperatures 700-800°C and it increases at 900-1000°C. Grain growth can contribute to this behaviour. For samples deformed at temperature 900°C and strain rate 10 and 50 s^{-1}, the recrystallized volume fraction is close to one. Samples deformed at 1000°C are fully recrystallized. It is expected that a character of relationship between grain size and process parameters shown in figure 2 is controlled by chromium precipitation at higher temperatures.

Conventional microstructure evolution model, based on the works of Sellars (1979), is applied. JAMK equation is used to model kinetics of static recrystallization:

$$X = 1 - \exp\left[\ln(0.5)\left(\frac{t}{t_{0.5}}\right)^{p}\right] \qquad (3)$$

$$t_{0.5} = A\varepsilon^{-m} D_0^{\,q} \dot{\varepsilon}^{-n} \exp\left(\frac{Q}{RT}\right) \qquad (4)$$

where: X – recrystallized volume fraction, t – time, $t_{0.5}$ – time for 50% static recrystallization, D_0 – grain size prior to deformation, ε – strain, $\dot{\varepsilon}$ – strain rate, p, A, m, q and n – coefficients, Q – activation energy.

Recrystallized grain size equation is:

$$D_{rx} = A\,\varepsilon^{-m} D_0^{q} \dot{\varepsilon}^{-n} \exp\left(-\frac{Q}{RT}\right) \qquad (5)$$

Finally, the following grain growth model is used:

$$D(t)^{q} = D_{rx}^{q} + At \exp\left(-\frac{Q}{RT}\right) \qquad (6)$$

Stress relaxation tests, which are described for example by Karjalainen and Perttu (1996), were used for identification of the microstructure evolution model. Typical stress relaxation plots corrected for the influence of the dynamic recovery are shown in figure 3 and they replicate the static recrystallization. Precipitation slows down this process what makes modelling difficult. Identification yielded the coefficients in equations (3) – (6) given in table 3. The Avrami exponent in equation (3) is $p = 0.8$.

Table 3. *Coefficients in equations (3) - (6) obtained from the stress relaxation tests.*

Model/equation	A	m	n	q	p	Q
$t_{0.5}$ – (3),(4)	$7.305 \cdot 10^{-14}$	0.7	0.6	1.8	0.6	200 000
D_{rx} – (5)	472	0.7	0.1	0.277	-	48 597
$D(t)$ – (6)	$3.059 \cdot 10^{26}$	-	-	6.2	-	429 920

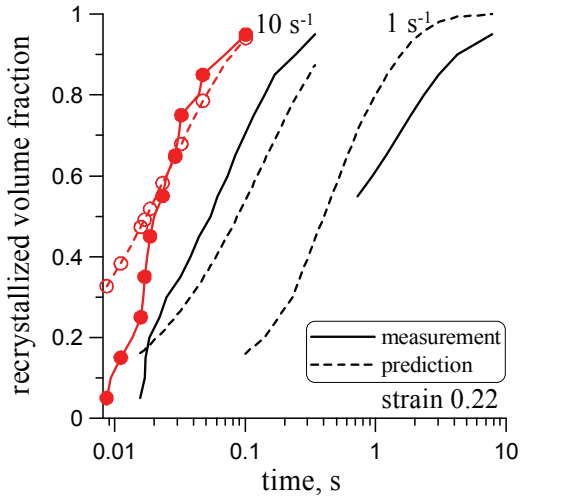

Fig. 3. *Comparison of the kinetics of the static recrystallization measured in the stress relaxation tests and calculated using equations (3) and (4), temperature 1000°C (with symbols) and 900°C (without symbols).*

Selected examples of the comparison of the kinetics of the static recrystallization measured in the tests and calculated using equations (3) and (4) are presented in figure 3. Similar comparison for the grain size (equations (5) and (6)) is shown in figure 4. Having in mind difficulties with interpretation of

the stress relaxation tests and measurement of grain size during static recrystallization, the accuracy of the microstructure evolution model can be considered reasonable. Developed model is implemented into the FE code and calculations of the grain size distribution in the volume of forgings during the whole process are performed.

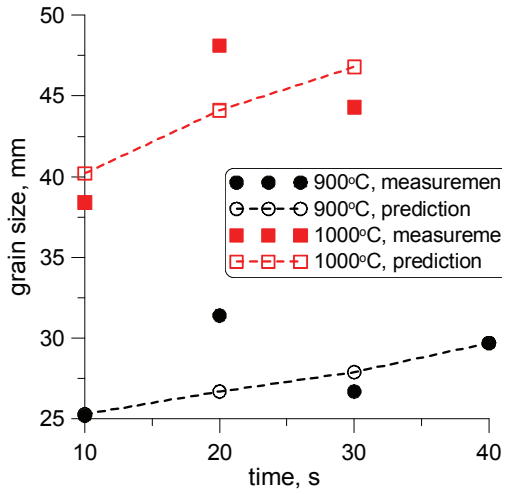

Fig. 4. *Comparison of the grain size measured in the tests and calculated using grain growth equations (5) and (6).*

2.4. Precipitation

In order to increase the strength, the Cu based alloys are subjected to ageing that is being conducted in the temperature range 450-550°C. The model of precipitation kinetics, adopted from Dutta et al. (2001), is described briefly below. More details are presented in Pietrzyk et al.'s work (2010b) and Deschamp's and Brecht's paper (1999). The model is composed of three sub-models, including: nucleation and growth, growth only and coarsening. The following parameters are to be determined:

– the driving force for precipitation

$$\Delta G_V = -\frac{RT}{V_m}\ln\left(\frac{C_{Cr}}{C^e_{Cr}}\right) \tag{7}$$

where: V_m – the molar volume of the precipitate, C_{Cr}, C^e_{Cr} – instantaneous and equilibrium concentrations of chromium calculated using the solubility product given by:

$$C^e_{Cr} = 1745\exp\left(-\frac{68686}{RT}\right) \tag{8}$$

– the critical radius for particles

$$r_c = -\frac{2\gamma}{\Delta G_v} \tag{9}$$

where: γ – the surface energy of the precipitate in the range of 0.2–0.3 J/m^2 for coherent and 0.5 J/m^2 for incoherent particles.

The interaction between dislocations and precipitates is based on the assumption that the dislocation core energy over the precipitate radius is spent for the nucleation. Thus, the activation energy, ΔG, for the formation of the critical nucleus of radius r_c, is the sum of the chemical free energy, the interfacial free energy and the dislocation core energy:

$$\Delta G = \pi\frac{16}{3}\frac{\gamma^3}{\Delta G_V^2} - 0.8\mu b^2\frac{\gamma}{\Delta G_V} \tag{10}$$

where: μ – the shear modulus, b – length of the Burgers vector of the matrix.

The variation in the volume fraction of precipitates is given by the nucleation rate, which is calculated as Deschamp and Brecht (1999):

$$\left.\frac{dN}{dt}\right|_{nucl} = N_0 Z\beta^*\exp\left(-\frac{\Delta G}{kT}\right)\exp\left(-\frac{\tau}{t}\right) \tag{11}$$

where: N_0 – number of available sites for either homogeneous or heterogeneous nucleation (estimated as $N_0 = 0.5\rho^{1.5}$ (Deschamp & Brecht, 1999), Z – the Zeldovich parameter (≈1/20), k – Boltzman constant, β^* – atomic impingement rate, τ – the incubation time defined as:

$$\beta^* = \frac{4\pi r_c^2 D C_{Cr}}{a_0^4} \qquad \tau = \frac{1}{2\beta^* Z}$$

where: D – the diffusivity, C_{Cr} – concentration of chromium in the solid solution, which is rate nucleation rate controlling factor, a_0 - the lattice constant of the matrix.

The evolution of the precipitate radius during the nucleation and growth stage is, respectively for nucleation and growth and for coarsening:

$$\left.\frac{dr}{dt}\right|_{nucl+growth} = \frac{1}{N}\frac{dN}{dt}\left[\alpha\frac{r_0}{\ln\left(\frac{C_{Cr}}{C^e_{Cr}}\right)} - r\right] + \frac{D}{r}\frac{C_{Cr} - C^e_{Cr}\exp\left(\frac{r_0}{r}\right)}{C^p_{Cr} - C^e_{Cr}\exp\left(\frac{r_0}{r}\right)}$$

$$r_0 = \frac{2\gamma V_m}{RT} \tag{12}$$

$$\left.\frac{dr}{dt}\right|_{coars} = \frac{4}{27}\frac{C^e_{Cr}}{C^p_{Cr} - C^e_{Cr}}\frac{r_0 D}{r} \tag{13}$$

where: α = 1.05 – the numerical factor accounting for the fact that nucleated precipitates can grow only if their radius is slightly larger than the critical one, C^p_{Cr} – concentration of Cr in the precipitate Superscript *e* stands for the equilibrium content of chromium in the solid solution – boundary limit.

In order to change continuously from the growth stage to the coarsening stage, the following coarsening function is defined:

$$\frac{dr}{dt} = (1 - f_{coars})\left.\frac{dr}{dt}\right|_{growth} + f_{coars}\left.\frac{dr}{dt}\right|_{coars} \tag{14}$$

$$\frac{dN}{dt} = f_{coars}\left.\frac{dN}{dt}\right|_{coars} \tag{15}$$

where:

$$f_{coars} = 1 - erf\left\{4\left[\frac{r}{r_0}\ln\left(\frac{C_{Cr}}{C^e_{Cr}}\right) - 1\right]\right\} \tag{16}$$

The volume fraction of particles f_v is given by the product of the number of particles and an average volume of a particle. The model is implemented in the FE code and used for simulations of the precipitation in the Cu based alloy. The contribution of the precipitation strengthening to the flow stress is calculated with the equation (Dutta et al., 2001):

$$\sigma_p = 0.691 kM\mu f_V^{0.5} \tag{17}$$

where volume fraction of precipitates is:

$$f_V = \frac{4}{3}\pi N r^3 \tag{18}$$

Precipitation strengthening is used to increase the strength of the Cu-Cr alloys.

3. SIMULATIONS

Simulations of forging of the Cu-Cr alloys, accounting for the microstructure evolution, were performed. Evaluation of the forging parameters and analysis of various variants of forging, as it is shown by Nowak et al. (2008), is the objective of simulations. Selected results of the simulations are shown below.

3.1. Hot forging

Various variants of manufacturing chains for five Cu-Cr forgings are investigated in Pietrzyk et al.'s works (2010a; 2010b) and the following schedule is proposed as the most efficient for these products: casting – hot extrusion – upsetting – forging – super saturation annealing - aging. Detailed parameters of subsequent processes are given by Pietrzyk et al. (2010b). Forging shown in figure 5 is selected in the present paper for demonstration of simulations of the microstructure evolution during this cycle.

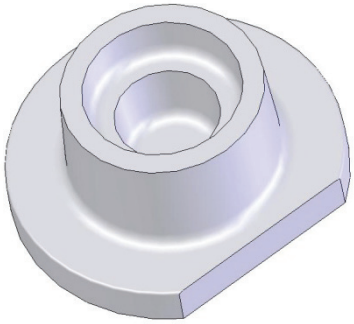

Fig. 5. *Forging investigated in the present work.*

Simulations were performed using Forge finite element code. Microstructure evolution model was implemented in this code and calculations of grain size were performed in each element of the mesh. In consequence, distribution of microstructural parameters in the volume of the forging was obtained. Full set of results of simulations including temperatures, strains, strain rates and stresses, as well as forces and die wear, can be found in Nowak et al.'s work (2008), Kuziak et al.'s work (2009), Pietrzyk et al.'s works (2010a; 2010b) and only results for the microstructure evolution are presented in this paper.

Casting and extrusion were not analysed. An average grain size after extrusion was 16 μm and it was taken as initial for the forging process. Processes of preheating and cooling to the deformation temperature of 900°C were analyzed next and the average grain size at the beginning of deformation was 20 μm. Distribution of the grain size at the cross section of the sample after upsetting is shown in figure 6. Distribution of the grain size at the cross section of the forging at subsequent stages of the process performed in 5 hits is shown in figure 7. Grain refinement is well seen in these plots, but then grain growth is observed after the last stage of forging. The grain size in the final product varies between 22 μm close to the surface to 28 μm in the

centre. It is confirmed by the micrographs taken from the forgings after the process (figure 8).

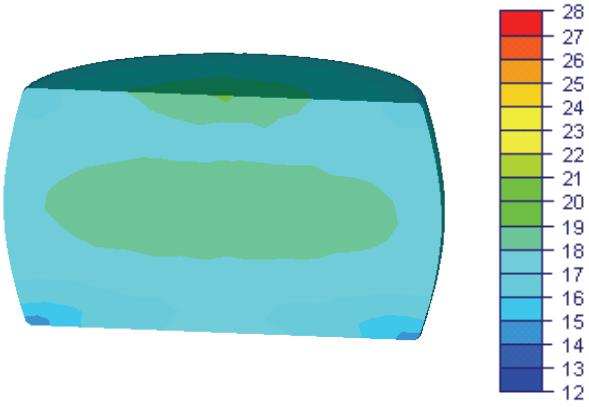

Fig. 6. *Distribution of the grain size at the cross section of the sample after upsetting.*

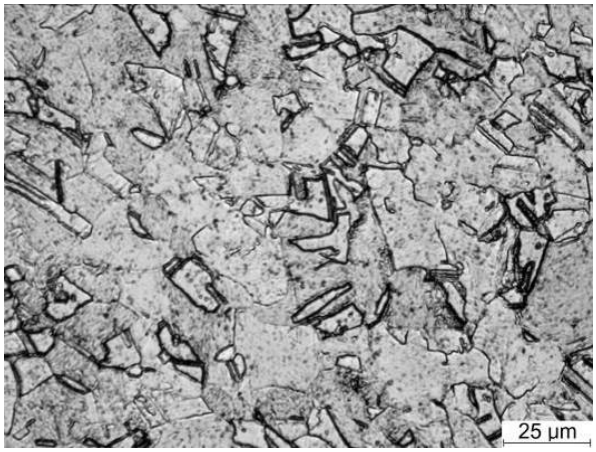

Fig. 8. *Microstructure at the centre of the sample after forging at 900°C and cooling to the room temperature.*

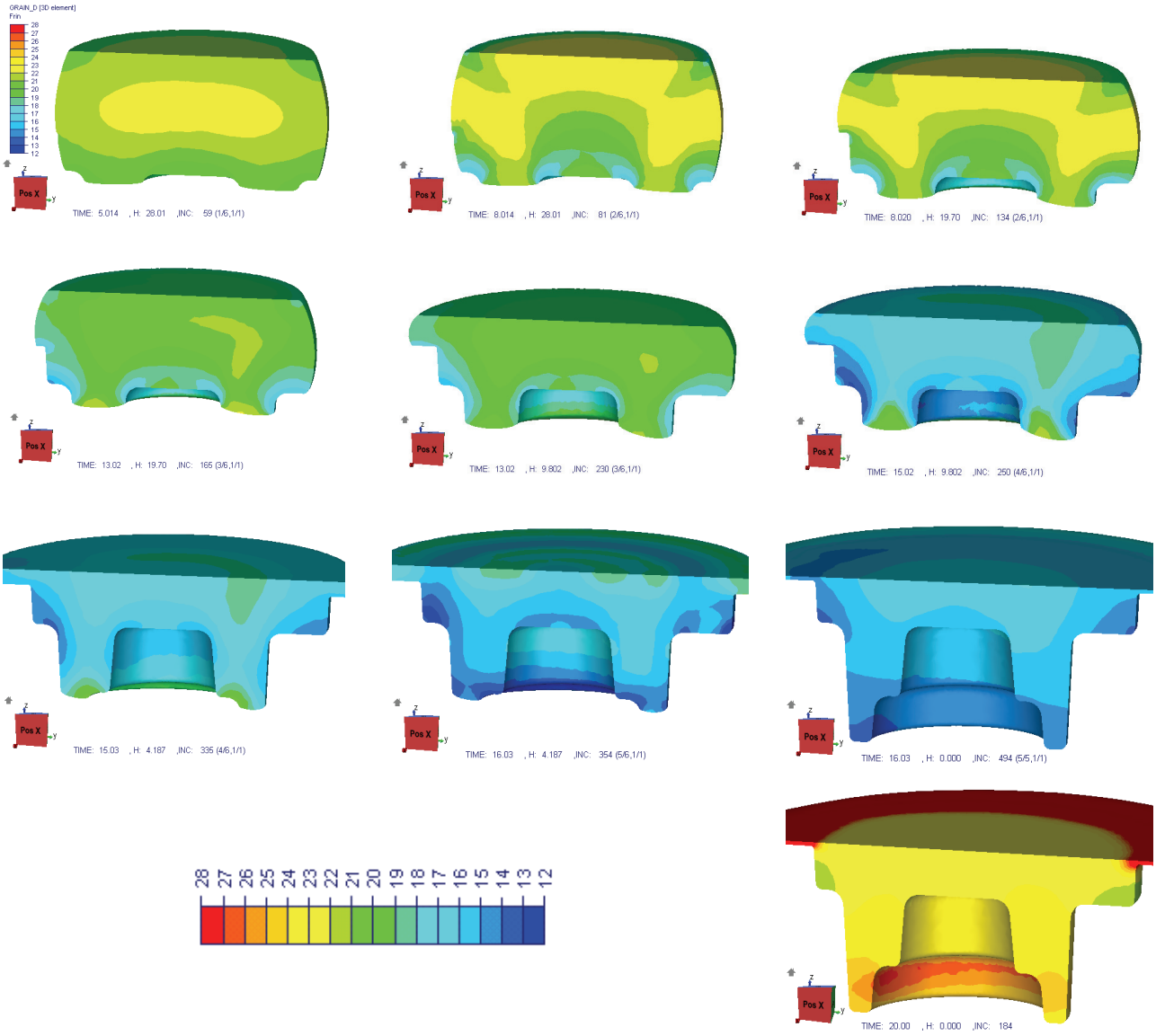

Fig. 7. *Distribution of the grain size at the cross section of the forging subsequently after the hit and before the next hit (5 stages) and 20 s after the last hit. Scale is the same in all figures.*

3.2. Super saturation annealing and ageing

Hardness of the sample after hot forging was at the level of 60 HV, which is below the required 100 HV. Therefore, additional heat treatment composed of super saturation annealing and ageing was applied to obtain hardening by precipitates. Simulations of the kinetics of the precipitation were performed using the model described in section 2.4 and selected result is presented in figure 9.

The influence of the chromium precipitates on the structure and the flow stress depends on the dispersion of this phase Dybiec et al. (1989). For small deformations, the presence of strongly dispersed particles favors a uniform dislocation distribution. A decrease in dispersion leads to cell structure formation and to strain localizations. Selected results of the TEM analysis are shown by Pietrzyk et al. (2010b). It is assumed that the size of precipitates around 4-6 nm gives good results as far as hardness is considered. Analysis of results of simulations of the heat treatment shows that these parameters should be obtained after ageing at 500°C for 3600 seconds.

Laboratory tests were performed to evaluate these predictions. All samples after forging were cut into 10 mm thick slices and they were subjected to various heat treatment schedules, see table 4. Hardness of the samples was measured and the average values with standard deviation are given in figure 10. It is seen that schedule HT3 gives the highest hardness and this schedule is included in the optimal manufacturing chain.

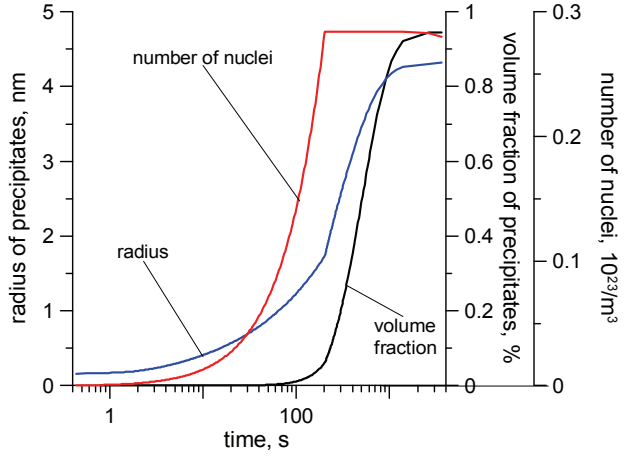

Fig. 9. *Results of simulations of the number of nuclei, average radius of precipitates and volume fraction of participates during aging after saturation annealing.*

Table 4. *Parameters of the heat treatment*

schedule	preheating		aging	
	T, °C	*t*, min	*T*,°C	*T*, min
HT1	500	30	-	-
HT2	1000	60	500	30
HT3	1000	60	500	60
HT4	-	-	500	30
HT5	-	-	450	30

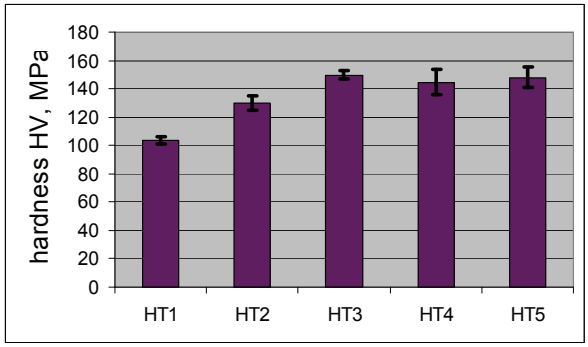

Fig. 10. *Average hardness and the standard deviation for investigated samples.*

4. CONCLUSIONS

Analysis of microstructure evolution during the optimal manufacturing cycle for the CuCr forgings proposed by Pietrzyk et al. (2010b) shows, that the process is properly designed and grain size at the level of 22-28 μm is obtained after hot forging. This does not yield the required hardness and additional heat treatment composed of super saturation annealing and ageing is applied. The optimal parameters of the heat treatment are preheating at 1000°C for 1 hour and ageing at 500°C for 1 hour (HT4 in table 4). Optimal parameters give the required hardness around 140 HV. This technology should be recommended when the press capacity is low. Other possibilities, including warm forging at the temperature range 450-600°C will be considered in the future.

ACKNOWLEDGEMENTS

Financial assistance of the MNiSzW, project R07 005 02, is acknowledged.

REFERENCES

Deschamp, A., Brecht, Y., 1999, Influence of predeformation and ageing of an Al-Zn-Mg alloy – II. Modelling of precipitation kinetics and yield stress, *Acta Mater.*, 47, 293-305.

Dutta, B., Palmiere, E.J., Sellars, C.M., 2001, Modelling the kinetics of strain induced precipitation in niobium microalloyed austenite, *Acta Mater*., 49, 785-794.

Dybiec, H., Rdzawski, Z., Richert, M., 1989, Flow stress and structure of age-hardened Cu-0.4%Cr alloy after large deformation, *Mat. Sci. Eng*., A108, 97-104.

Gavrus, A., Massoni, E., Chenot, J.L., 1996, An inverse analysis using a finite element model for identification of rheological parameters, *J. Mat. Proc. Techn*., 60, 447-454.

Karjalainen, L.P., Perttu, J., 1996, Characteristics of static and metadynamic recrystallization strain accumulation in hot deformed austenite as revealed by stress relaxation method, *ISIJ International*, 36, 729-736.

Kumar, S., Singh, T.P., 2007, A comparative study of the performance of different EDM electrode materials in two dielectric media, *IE(I) Journal-PR*, 87, 3-8.

Kuziak, R., Pidvysotskyy, V., Drozdowski, K., 2009, Validation of the thermo-mechanical-microstructural model of hot forging process, *Computer Methods in Material Science*, 9, 424-434.

Nowak, J., Węglarczyk, S., Kuziak, R., Drozdowski, K., Pietrzyk, M., 2008, Computer aided design of manufacturing technology for copper-chromium alloys, *Computer Methods in Material Science*, 8, 186-195.

Pietrzyk, M., Kuziak, R., 2009, Naprężenie uplastyczniające stopów miedzi z chromem odkształcanych na gorąco dla temperatur i prędkości odkształcenia występujących w procesie kucia, *Rudy Metale*, 54, 208-216 (in Polish).

Pietrzyk, M., Madej, Ł., Kuziak, R., 2010a, Optimal design of manufacturing chain based on forging for copper alloys, with product properties being the objective function, *CIRP Annals - Manufacturing Technology*, 59, 319–322.

Pietrzyk, M., Kuziak, R., Pidvysotskyy, V., Nowak, J., Węglarczyk, S., Drozdowski, K., 2010b, Computer aided technology design for forging of CuCr alloys, *Polish Metallurgy 2006-2010 in time of the worldwide economic crises*, ed., Świątkowski K., Komitet Metalurgii PAN, Kraków, 147-169.

Report, 1998, High conductivity coppers for electrical engineering, *Copper Development Association Publication 122*.

Sellars, C.M., 1979, Physical metallurgy of hot working, *Hot working and forming processes*, eds, Sellars, C.M., Davies, G.J., The Metals Soc., London, 3-15.

Szeliga, D., Gawąd, J., Pietrzyk, M., 2006, Inverse analysis for identification of rheological and friction models in metal forming, *Comp. Meth. Appl. Mech. Engrg*., 195, 6778-6798.

DOBÓR NAJLEPSZYCH PARAMETRÓW OBRÓBKI CIEPLNO-MECHANICZNEJ DLA WYTWARZANIA ODKUWEK ZE STOPU CuCr

Streszczenie

Celem pracy jest uwzględnienie rozwoju mikrostruktury w projektowaniu technologii wytwarzania odkuwek ze stopów na bazie miedzi. Jako przykład wybrano stop miedzi z chromem (CuCr). W pracy podano podstawowe własności cieplne, elektryczne i mechaniczne stopu, które porównano z danymi dla czystej miedzi i stali. Ocena wpływu starzenia i procesu wydzieleniowego na własności stopu jest jednym z celów pracy. Przeprowadzono próby plastometryczne i relaksacji naprężeń dla różnych temperatur i prędkości odkształcenia. Zastosowano różne schematy wygrzewania próbek, co pozwoliło na ocenę wpływu początkowej mikrostruktury na zachowanie się stopu. Opracowano model reologiczny i model rozwoju mikrostruktury i przeprowadzono weryfikację tych modeli. Modele zaimplementowano w programie z metody elementów skończonych (MES) i wykonano symulacje rozwoju mikrostruktury w czasie całego cyklu produkcji oraz obliczenia własności wyrobów. Połączenie programu MES z modelami reologicznym i mikrostrukturalnym stworzyło narzędzie umożliwiające analizowanie różnych wariantów cyklu produkcji dla wyrobów z miedzi chromowej.

Received: November 22, 2010
Received in a revised form: November 25, 2010
Accepted: November 26, 2010